

Communication

High-Speed Laser Metal Deposition of CrFeCoNi and AlCrFeCoNi HEA Coatings with Narrow Intermixing Zone and Their Machining by Turning and Diamond Smoothing

Thomas Lindner ^{1,*} , Hendrik Liborius ², Gerd Töberling ³, Sabrina Vogt ⁴, Bianca Preuß ¹, Lisa-Marie Rymer ¹ ,
Andreas Schubert ²  and Thomas Lampke ¹ 

- ¹ Materials and Surface Engineering Group, Institute of Materials Science and Engineering, Chemnitz University of Technology, 09107 Chemnitz, Germany; bianca.preuss@mb.tu-chemnitz.de (B.P.); lisa-marie.rymer@mb.tu-chemnitz.de (L.-M.R.); thomas.lampke@mb.tu-chemnitz.de (T.L.)
- ² Professorship Micromanufacturing Technology, Institute for Machine Tools and Production Processes, Chemnitz University of Technology, 09107 Chemnitz, Germany; hendrik.liborius@mb.tu-chemnitz.de (H.L.); andreas.schubert@mb.tu-chemnitz.de (A.S.)
- ³ Fraunhofer Institute for Machine Tools and Forming Technology IWU, 09126 Chemnitz, Germany; gerd.toeberling@iwu.fraunhofer.de
- ⁴ TRUMPF Laser- und Systemtechnik GmbH, 71254 Ditzingen, Germany; sabrina.vogt@trumpf.com
- * Correspondence: th.lindner@mb.tu-chemnitz.de



Citation: Lindner, T.; Liborius, H.; Töberling, G.; Vogt, S.; Preuß, B.; Rymer, L.-M.; Schubert, A.; Lampke, T. High-Speed Laser Metal Deposition of CrFeCoNi and AlCrFeCoNi HEA Coatings with Narrow Intermixing Zone and Their Machining by Turning and Diamond Smoothing. *Coatings* **2022**, *12*, 879. <https://doi.org/10.3390/coatings12070879>

Academic Editor: Hideyuki Murakami

Received: 12 May 2022
Accepted: 20 June 2022
Published: 21 June 2022

Publisher's Note: MDPI stays neutral with regard to jurisdictional claims in published maps and institutional affiliations.



Copyright: © 2022 by the authors. Licensee MDPI, Basel, Switzerland. This article is an open access article distributed under the terms and conditions of the Creative Commons Attribution (CC BY) license (<https://creativecommons.org/licenses/by/4.0/>).

Abstract: The processing of high-entropy alloys (HEAs) via laser metal deposition (LMD) is well known. However, it is still difficult to avoid chemical intermixing of the elements between the coating and the substrate. Therefore, the produced coatings do not have the same chemical composition as the HEA feedstock material. Single-layer CrFeCoNi and AlCrFeCoNi HEA coatings were deposited using high-speed laser metal deposition (HS-LMD). Elemental mapping confirmed a good agreement with the chemical composition of the powder feedstock material, and revealed that chemical intermixing was confined to the immediate substrate interface. The coatings are characterized by a homogeneous structure with good substrate bonding. The machining of these coatings via turning is possible. Subsequent diamond smoothing results in a strong decrease in the surface roughness. This study presents a complete manufacturing chain for the production of high-quality HS-LMD HEA coatings.

Keywords: coating; diamond smoothing; HEA; HS-LMD; LMD; machining; turning

1. Introduction

High-entropy alloys (HEAs) are increasingly being used as feedstocks for different coating processes [1–4]. The limitation of material usage allows these comparatively expensive materials to be used for corrosion or wear protection applications. In the field of cladding processes, laser metal deposition (LMD) technology dominates [5–8]. Currently, laser focusing on the substrate to form a molten pool is predominantly used [9–11]. This leads to a strong mixing of the substrate and the coating material. The requirement for the integrity of the chemical composition of HEAs is therefore not sufficiently fulfilled. Increasing the traverse speed can prevent this [12]. Although the gradient is reduced by multilayer coating, reproducible results are rarely achieved. Focusing the laser beam above the substrate surface represents a suitable alternative approach that has hardly been considered so far [13]. The powder feedstock material is thus melted above the substrate and is applied to an only slightly melted substrate. Hence, metallurgical mixing is largely prevented. Although surface treatment is an essential step in the conditioning of functional surfaces, the finishing of HEAs is only rarely reported. Furthermore, the machining of HEA coatings by turning and diamond smoothing is analyzed in a few papers [14–18]. Especially, the machining of laser clad HEA coatings has not been investigated so far.

The deposition of the CrFeCoNi and AlCrFeCoNi HS-LMD coatings and the mechanical finishing by turning and diamond smoothing represent the complete manufacturing chain under consideration of the material behavior. Therefore, this paper contributes to an improved knowledge of HEA coating systems, and therefore, it generally enables an increase in the field of applications of HEAs.

2. Materials and Methods

Feedstocks of the equimolar HEAs CrFeCoNi and AlCrFeCoNi were produced using inert gas atomization, and they were subsequently classified to adjust a particle size range of $-45 +15 \mu\text{m}$. Laser metal deposition (LMD) was performed using a high-speed laser cladding system (HS-LMD), consisting of a TRUMPF BEO D70 Optic equipped with the prototype of a TRUMPF 7-ray nozzle and a TRUMPF TruDisk 6001 laser source. With a spot width of approximately 2 mm, the focal point was 1.5 mm above the substrate surface. A line offset of 300 μm and a traverse speed of 30 m/min were used. AISI304 grade steel discs with a diameter of 100 mm and a thickness of 6 mm were used as the substrate material.

The machining investigations were conducted on a precision lathe SPINNER type PD 32. The coating systems were post-processed via face turning and partial subsequent diamond smoothing. The machining of these coatings was necessary to reduce the comparatively high initial surface roughness (surface roughness depth $R_z > 100 \mu\text{m}$). Using subtractive processes, it is also possible to compensate for the geometrical errors of the specimens, such as deviations in evenness due to the temperature impact during the coating process. For turning the CBN-tipped indexable inserts of the geometry CCGW 09T304, those characterized by a rake angle of 0° and a sharp cutting edge (radius $< 10 \mu\text{m}$) were used. In combination with the tool holder used, the cutting-edge angle of the minor cutting edge was 5° . The cutting material consisted of 90–95% boron nitride, characterized by a grain size of approximately 1 μm bounded by cobalt. Dry machining via face turning was performed at a constant cutting speed (200 m/min), feed (0.05 mm), and depth of cut (0.1 mm). Part of the turned samples was subsequently machined via diamond smoothing, with a smoothing force of 100 N, a speed of 70 m/min, and a feed of 0.025 mm, using a spherical monocrystalline diamond tool characterized by a radius of 2 mm. To improve the sliding behavior, emulsion flood cooling was used.

The topography of the machined coatings was analyzed using 3D laser scanning microscopy (3D LSM) using Keyence VK9700 (Keyence, Osaka, Japan). Image sections of size 1 mm \times 1 mm were recorded at different points of the machined coating surfaces. Additionally, tactile measurements were performed in the direction of the feed motion with a stylus instrument, Mahr type LD120 (Mahr, Göttingen, Germany). The stylus was characterized by a radius of 2 μm . The determination and evaluation of the surface profiles was performed in accordance with DIN EN ISO 11562. For each specimen, five measurements were performed at different points on the machined coating surface to determine fluctuations in the measured values and differences in the surface properties. The feedstock material was investigated via scanning electron microscopy (SEM), using a Zeiss LEO 1455VP microscope (Zeiss, Jena, Germany). The coatings were investigated using an optical microscope, GX51, equipped with a SC50 camera. Beraha II etchant was used to contrast the substrate and coating material in cross-sectional view. The chemical composition within the immediate substrate interface was measured using energy-dispersive X-ray spectroscopy (EDS) with an EDAX EDS GENESIS system.

3. Results

The SE images in Figure 1 reveal that the feedstock powder exhibited a spherical morphology. A small degree of inner porosity was proven in cross-sectional view. Both powders showed good flow properties and could be processed continuously in the HS-LMD system. After a single coating step, the average coating thickness was approximately 350 μm . Due to mechanical finishing, this was reduced to approximately 200 μm . The cross-section micrographs in the etched state demonstrated good substrate adhesion for

both HEAs, with minor porosity within the coating (Figure 1). In the case of AlCrFeCoNi, a clear color deposition appeared, which allowed for a good visualization of a trace overlap. A clear contrast between the substrate and the coating material revealed a limited degree of intermixing.

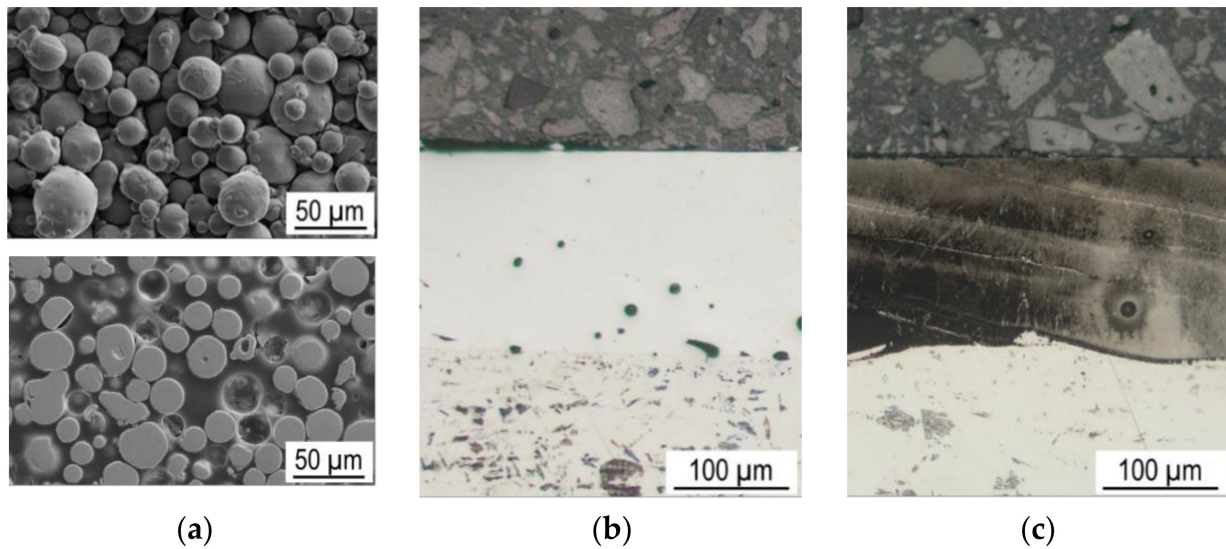


Figure 1. SE images of a feedstock material, as well as optical microscope images of the diamond smoothed HS-LMD coating systems in cross-sectional view after etching. (a) CrFeCoNi powder, (b) CrFeCoNi coating, (c) AlCrFeCoNi coating.

The results of the EDS linescan measurements in the interface between the substrate and the coating materials in Figure 2 could confirm this. For both alloys, the gradient region was less than 10 μm. In the case of the AlCrFeCoNi coating, a reincrease in the Fe concentration was observed for an interface distance of approximately 20 μm. This can be attributed to the depositions of substrate at the interface in the trace overlap region. With a further increase in interfacial distance, no elemental variations were observed in either coating system.

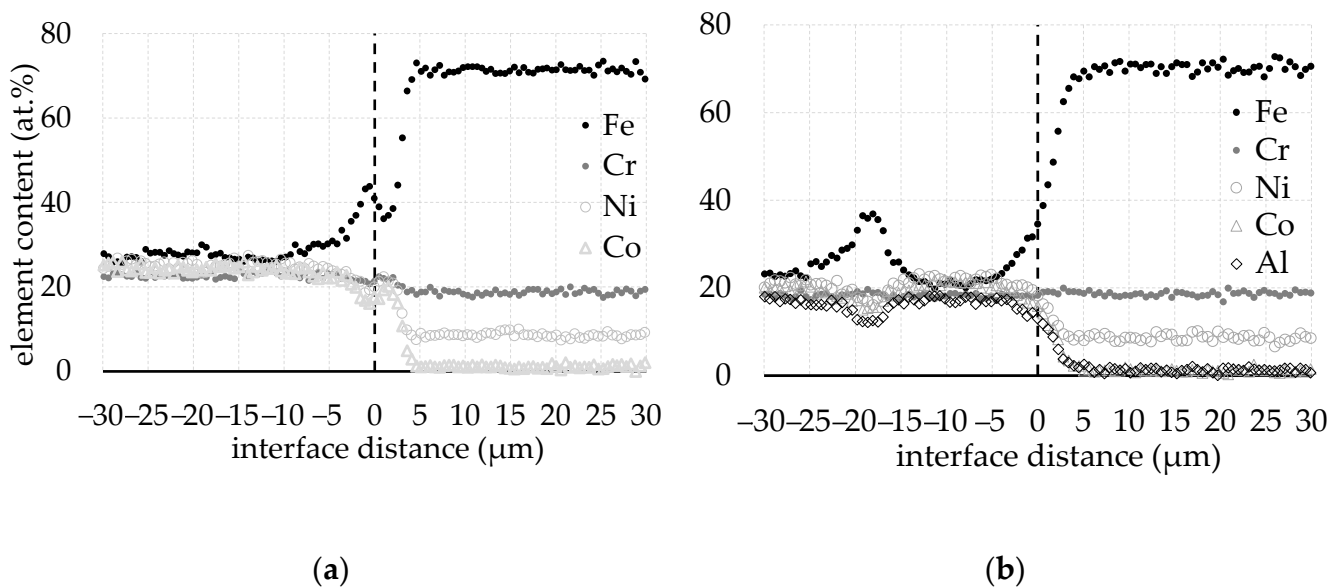


Figure 2. EDS elemental mapping within the transition area between HS-LMD coating and substrate material. (a) CrFeCoNi coating, (b) AlCrFeCoNi coating.

Furthermore, comparative measurements on the powder feedstocks showed good agreement in the chemical composition (Table 1). A slight decrease in the concentrations of Al and Cr was observed in the coating system. The elemental composition determined at the surface of the coating showed good agreement with the composition determined in the near-interface region. This confirms the limited chemical mixing and indicates a slight vanishing of the oxygen affinity alloy constituents.

Table 1. Chemical composition of atomized powder and HS-LMD coating in at.%, measured using EDS.

Sample		Al	Cr	Fe	Co	Ni
CrFeCoNi	Powder	-	25.7	25.0	24.6	24.7
	Coating	-	23.5	25.7	25.4	25.4
AlCrFeCoNi	Powder	20.7	19.7	19.9	20.0	19.7
	Coating	18.0	18.8	19.8	21.8	21.6

Due to the surface roughness, after HS-LMD processing, the coatings were machined via face turning. The detected mean values for R_a (arithmetic mean surface roughness) and R_z (surface roughness depth) are shown in Figure 3. The machining of both coating systems resulted in comparatively high surface roughness values of the turned samples, and a strong difference in the calculated kinematic roughness ($R_{z_{kin}} = 0.78 \mu\text{m}$). Surface roughness values after turning were similar for both coating systems. The high roughness values were explained by the comparatively high tool wear, resulting in deviations from the kinematic roughness profile. Additionally, the cutting-edge geometry seemed to be unsuitable for machining laser clad coatings, as the HS-LMD coating was partially smeared or severely deformed during turning, instead of being cut. This resulted in a comparatively high surface roughness ($R_z < 4.2 \mu\text{m}$), and clearly differed from previous work on the thermal spray HEA coatings with a ($R_z < 1.8 \mu\text{m}$) after turning [15].

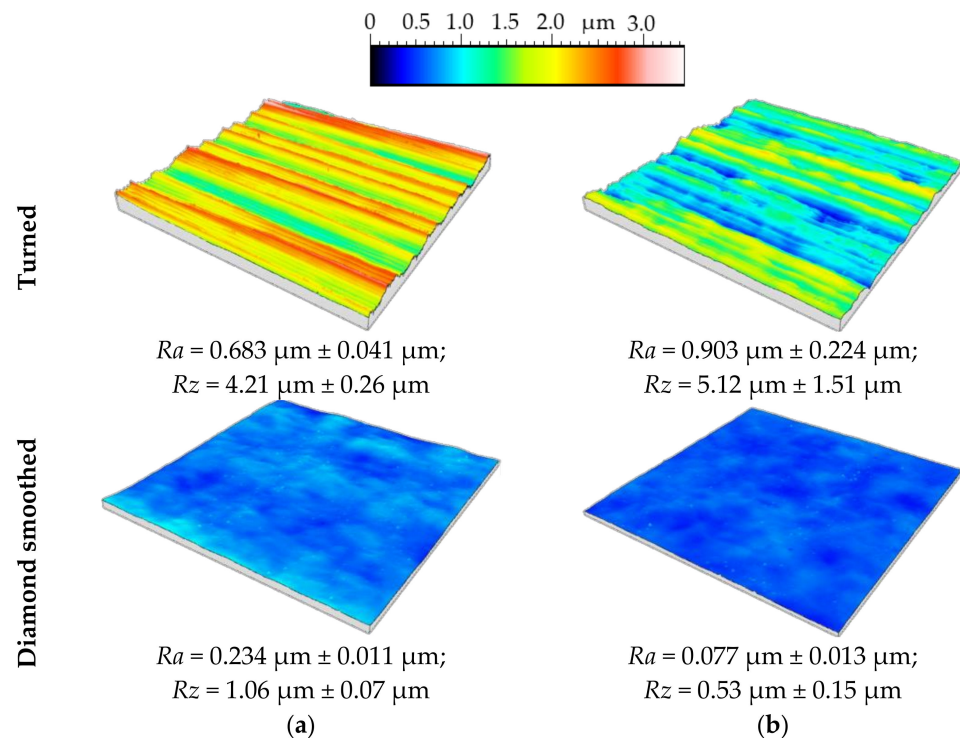


Figure 3. Micrographs, detected using 3D LSM, of the HS-LMD HEA coating surfaces after machining (size $1 \text{ mm} \times 1 \text{ mm}$) with characteristic roughness values (detected via tactile measurements). (a) CrFeCoNi coating, (b) AlCrFeCoNi coating.

A comparison of the two coating processes shows that the constitution of the coating had a stronger influence on the results of the turning process than did the chemical composition. Subsequent diamond smoothing of the LMD coatings significantly reduced the surface roughness values by deforming the peaks and lifting the valleys of the turned surface profile. However, the mean values for Ra were three-fold, and for Rz , two-fold higher after smoothing the CrFeCoNi HEA, compared to the other coating. The 3D LSM images show that the smoothing force was too high in the case of CrFeCoNi. Hence, there was a deformation of the profile peaks after turning, as well as the appearance of a kind of kinematic surface profile, due to diamond smoothing. Reducing the smoothing force can provide roughness values that are similar to those of the AlCrFeCoNi coating system. Compared to alternative mechanical processing methods such as grinding, electrical discharge machining, or milling on selective laser-melted CoCrFeMnNi parts, significantly lower surface roughness values are possible with diamond smoothing [16].

4. Summary

A complete manufacturing chain for the HS-LMD of CrFeCoNi and AlCrFeCoNi HEA coatings was presented. Limited heating of the substrate successfully reduces metallurgical mixing. In addition, only a minor decrease in the concentration of the oxygen affine elements Al and Cr was detectable for the coating system. The coating surfaces can be machined effectively by turning, while diamond smoothing leads to a significant reduction in surface roughness. The successful deposition of single-layer coatings via HS-LMD and their subsequent machining show the application potential of the presented manufacturing chain.

Author Contributions: Conceptualization, T.L. (Thomas Lindner), H.L. and G.T.; methodology, T.L. (Thomas Lindner), H.L. and G.T.; validation and investigation, T.L. (Thomas Lindner), H.L., L.-M.R., S.V. and B.P.; writing—original draft preparation, T.L. (Thomas Lindner) and H.L.; writing—review and editing, and supervision, A.S. and T.L. (Thomas Lampke); project administration, T.L. (Thomas Lindner), A.S. and T.L. (Thomas Lampke); funding acquisition, T.L. (Thomas Lindner). All authors have read and agreed to the published version of the manuscript.

Funding: The study was funded via Sächsische Aufbaubank—Förderbank/SAB-100382175 by the European Social Fund ESF and the Free State of Saxony. The APC was funded by Chemnitz University of Technology.



Diese Maßnahme wird mitfinanziert durch Steuermittel auf der Grundlage des vom Sächsischen Landtag beschlossenen Haushaltes.

Institutional Review Board Statement: Not applicable.

Informed Consent Statement: Not applicable.

Data Availability Statement: Not applicable.

Acknowledgments: The support by Robert Glaßmann and Paul Seidel (all from the Institute of Materials Science and Engineering) is gratefully acknowledged.

Conflicts of Interest: The authors declare no conflict of interest.

References

1. Meghwal, A.; Anupam, A.; Murty, B.S.; Berndt, C.C.; Kottada, R.S.; Ang, A.S.M. Thermal Spray High-Entropy Alloy Coatings: A Review. *J. Therm. Spray Technol.* **2020**, *29*, 857–893. [[CrossRef](#)]
2. Löbel, M.; Lindner, T.; Kohrt, C.; Lampke, T. Processing of AlCoCrFeNiTi High Entropy Alloy by Atmospheric Plasma Spraying. *IOP Conf. Ser. Mater. Sci. Eng.* **2017**, *181*, 012015. [[CrossRef](#)]
3. Schwarz, H.; Uhlig, T.; Rösch, N.; Lindner, T.; Ganss, F.; Hellwig, O.; Lampke, T.; Wagner, G.; Seyller, T. CoCrFeNi High-Entropy Alloy Thin Films Synthesised by Magnetron Sputter Deposition from Spark Plasma Sintered Targets. *Coatings* **2021**, *11*, 468. [[CrossRef](#)]
4. Arif, Z.U.; Khalid, M.Y.; Rashid, A.A.; ur Rehman, E.; Atif, M. Laser deposition of high-entropy alloys: A comprehensive review. *Opt. Laser Technol.* **2022**, *145*, 107447. [[CrossRef](#)]

5. Li, J.; Huang, Y.; Meng, X.; Xie, Y. A Review on High Entropy Alloys Coatings: Fabrication Processes and Property Assessment. *Adv. Eng. Mater.* **2019**, *21*, 1900343. [[CrossRef](#)]
6. Arif, Z.U.; Khalid, M.Y.; ur Rehman, E.; Ullah, S.; Atif, M.; Tariq, A. A Review on Laser Cladding of High-Entropy Alloys, Their Recent Trends and Potential Applications. *J. Manuf. Processes* **2021**, *68*, 225–273. [[CrossRef](#)]
7. Lin, D.; Zhang, N.; He, B.; Zhang, G.; Zhang, Y.; Li, D. Tribological Properties of FeCoCrNiAl_x High-Entropy Alloys Coating Prepared by Laser Cladding. *J. Iron Steel Res. Int.* **2017**, *24*, 184–189. [[CrossRef](#)]
8. Shu, F.Y.; Zhang, B.L.; Liu, T.; Sui, S.H.; Liu, Y.X.; He, P.; Liu, B.; Xu, B.S. Effects of laser power on microstructure and properties of laser cladded CoCrBFeNiSi high-entropy alloy amorphous coatings. *Surf. Coat. Technol.* **2019**, *358*, 667–675. [[CrossRef](#)]
9. Cui, C.; Wu, M.; Miao, X.; Zhao, Z.; Gong, Y. Microstructure and Corrosion Behavior of CeO₂/FeCoNiCrMo High-Entropy Alloy Coating Prepared by Laser Cladding. *J. Alloys Compd.* **2022**, *890*, 161826. [[CrossRef](#)]
10. Zhao, P.; Li, J.; Lei, R.; Yuan, B.; Xia, M.; Li, X.; Zhang, Y. Investigation into Microstructure, Wear Resistance in Air and NaCl Solution of AlCrCoNiFeTax High-Entropy Alloy Coatings Fabricated by Laser Cladding. *Coatings* **2021**, *11*, 358. [[CrossRef](#)]
11. Zhang, H.; He, Y.Z.; Pan, Y.; He, Y.S.; Shin, K.S. Synthesis and Characterization of NiCoFeCrAl₃ High Entropy Alloy Coating by Laser Cladding. *Adv. Mater. Res.* **2010**, *97*, 1408–1411. [[CrossRef](#)]
12. Wang, H.; Zhang, W.; Peng, Y.; Zhang, M.; Liu, S.; Liu, Y. Microstructures and Wear Resistance of FeCoCrNi-Mo High Entropy Alloy/Diamond Composite Coatings by High Speed Laser Cladding. *Coatings* **2020**, *10*, 300. [[CrossRef](#)]
13. Lindner, T.; Günen, A.; Töberling, G.; Vogt, S.; Karakas, M.S.; Löbel, M.; Lampke, T. Boriding of Laser-Clad Inconel 718 Coatings for Enhanced Wear Resistance. *Appl. Sci.* **2021**, *11*, 1935. [[CrossRef](#)]
14. Huang, Z.; Dai, Y.; Li, Z.; Zhang, G.; Chang, C.; Ma, J. Investigations on surface morphology and crystalline phase deformation of Al₈₀Li₅Mg₅Zn₅Cu₅ high-entropy alloy by ultra-precision cutting. *Mater. Des.* **2020**, *186*, 108367. [[CrossRef](#)]
15. Liborius, H.; Nestler, A.; Löbel, M.; Lindner, T.; Uhlig, T.; Schubert, A.; Wagner, G.; Lampke, T. Influence of the Composition of Thermally Sprayed (Al)CoCrFeNi(Mo) High-Entropy Alloy Coatings in Face Turning and Diamond Smoothing. In Proceedings of the 21st EUSPEN, Virtual, 7–10 June 2021; pp. 347–350, ISBN 978-0-9957751-9-0.
16. Guo, J.; Goh, M.; Zhu, Z.; Lee, X.; Nai, M.L.; Wei, J. On the machining of selective laser melting CoCrFeMnNi high-entropy alloy. *Mater. Des.* **2018**, *153*, 211–220. [[CrossRef](#)]
17. Clauß, B.; Liborius, H.; Lindner, T.; Löbel, M.; Schubert, A.; Lampke, T. Influence of the cutting parameters on the surface properties in turning of a thermally sprayed AlCoCrFeNiTi coating. *Procedia CIRP* **2020**, *87*, 19–24. [[CrossRef](#)]
18. Richter, T.; Arroyoa, D.D.; Börner, A.; Schröpfer, D.; Rhode, M.; Lindner, T.; Löbel, M.; Preuß, B.; Lampke, T. Ultrasonic assisted milling of a CoCrFeNi medium entropy alloy. *Procedia CIRP* **2022**, *108*, 879–884. [[CrossRef](#)]